Energy & Environmental Science

www.rsc.org/ees

Volume 5 | Number 2 | February 2012 | Pages 5461–5856

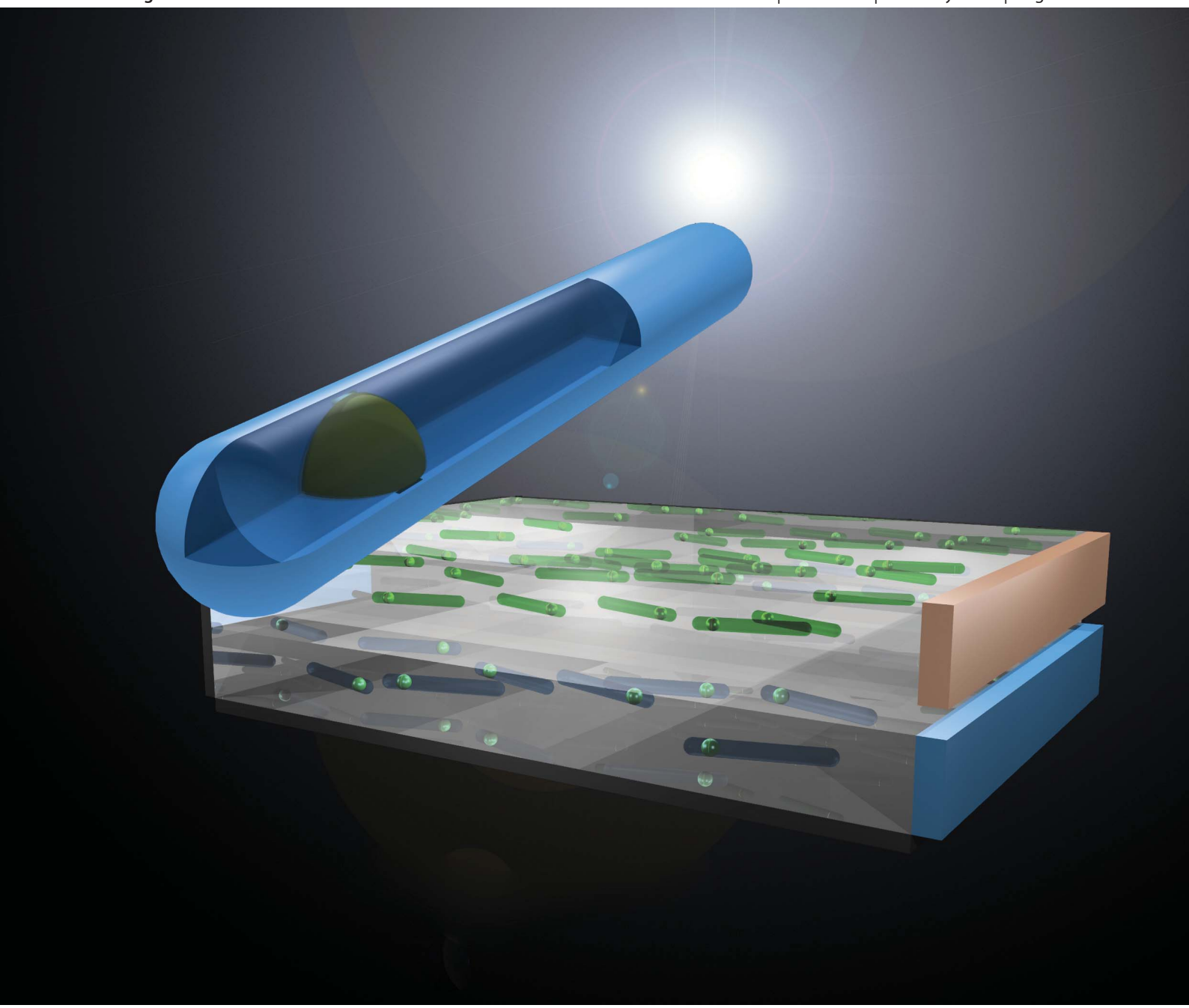

ISSN 1754-5692

RSC Publishing

COVER ARTICLE
Holt *et al.*
Optimizing luminescent solar concentrator design

1754-5692(2012)5:2;1-4

Energy & Environmental Science

Dynamic Article Links

Cite this: *Energy Environ. Sci.*, 2012, **5**, 5798

www.rsc.org/ees

PAPER

Optimizing luminescent solar concentrator design†

Hermilo Hernandez-Noyola,[a] David H. Potterveld,[a] Roy J. Holt*[a] and Seth B. Darling[b]

Received 15th August 2011, Accepted 26th October 2011
DOI: 10.1039/c1ee02376d

Luminescent Solar Concentrators (LSCs) use fluorescent materials and light guides to convert direct and diffuse sunlight into concentrated wavelength-shifted light that produces electrical power in small photovoltaic (PV) cells with the goal of significantly reducing the cost of solar energy utilization. In this paper we present an optimization analysis based on the implementation of a genetic algorithm (GA) subroutine to a numerical ray-tracing Monte Carlo model of an LSC, SIMSOLAR-P. The initial use of the GA implementation in SIMSOLAR-P is to find the optimal parameters of a hypothetical "perfect luminescent material" that obeys the Kennard Stepanov (K-S) thermodynamic relationship between emission and absorption. The optimization balances the efficiency losses in the wavelength shift and PV conversion with the efficiency losses due to re-scattering of light out of the collector. The theoretical limits of efficiency are provided for one, two and three layer configurations; the results show that a single layer configuration is far from optimal and adding a second layer in the LSC with wavelength shifted material in the near infrared region significantly increases the power output, while the gain in power by adding a third layer is relatively small. The results of this study provide a theoretical upper limit to the performance of an LSC and give guidance for the properties required for luminescent materials, such as quantum nanocrystals, to operate efficiently in planar LSC configurations.

Introduction

The LSC concept[1,2] is based on a planar device in which a fraction of the direct or diffuse sunlight, entering through the top of a transparent medium (plastic or glass), is converted to fluorescent light by luminescent materials deposited on top of or embedded within the medium. Eventually, this fluorescent light, following a total internal reflection mechanism, reaches a photovoltaic cell attached to one or more edges of the light guide material as shown schematically in Fig. 1.

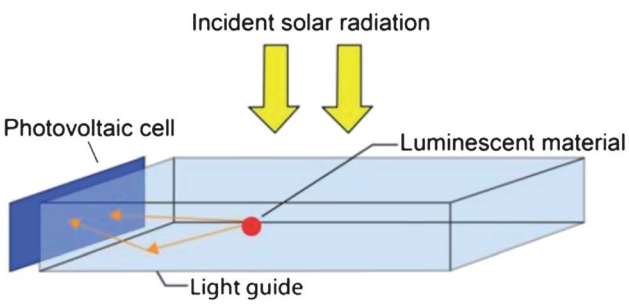

Fig. 1 Concept of a Luminescent Solar Concentrator (adapted from ref. 3).

[a] *Argonne National Laboratory, Physics Division, 9700 South Cass Avenue, Argonne, IL, USA. E-mail: holt@anl.gov; Fax: +01-630-252-3903; Tel: +01-630-252-4101*

[b] *Argonne National Laboratory, Center for Nanoscale Materials, 9700 South Cass Avenue, Argonne, IL, USA*

† Electronic supplementary information (ESI) available: Genetic algorithms implementation. See DOI: 10.1039/c1ee02376d

Broader context

Dramatically increasing utilization of solar energy will require significant reductions in cost. Luminescent solar concentrators represent one promising approach to such reductions because they can capture sunlight—including diffuse light—over a large area using low-cost materials and redirect that light onto much smaller solar cells. Moreover, the solar spectrum can be segmented by using stacked concentrators and bandgap-matched photovoltaics to increase conversion efficiency. The parameter space in luminescent solar concentrator design, however, is vast, and optimizing their performance empirically is a daunting challenge. Here we present a simulation-based approach that can focus experimental efforts in both materials and device design. With such guidance in hand, synthetic work will be more efficient and performance maximized. Future incorporation of cost models will further enhance the power of this approach.

This journal is © The Royal Society of Chemistry 2012

The advantages of LSCs include:

• The use of static concentrators without the need for costly and complex mobile or sun-tracking mechanisms.

• The capability to convert both direct and diffuse sunlight into electricity. An LSC can operate efficiently in diffuse sunlight as required for northern climates.

• High concentration ratios (the ratio between the area of the top surface to that of one edge of the device) reduce the area of the PV material.

• Because of the reduced area of PV material, a reduction of the PV material cost per unit energy generated can be achieved.

LSCs are effective in direct and diffuse light and can reduce the materials cost per watt of generated power by dramatically reducing the size of the PV cells. Efficient operation places severe constraints on the efficiency and optical properties of the luminescent medium. Organic dyes can meet these constraints, but only over a limited spectral range. A recent breakthrough in the LSC approach showed that a high-efficiency, solar-stable combination dye with a large Stokes shift could be used in a light guide medium to generate electrical power.[4] Another strategy of replacing the dyes with highly luminescent quantum nanocrystals[5,6] is attractive, because nanocrystals offer great photostability, wide spectral coverage and emission-absorption spectra that can be separately adjusted by varying the quantum nanocrystal dimensions and materials, all while maintaining solution processability.[7] The intent of this study is to determine the theoretical operational limits of an LSC and provide guidance for the luminescent properties required of quantum nanocrystals to be used as luminescent materials.

Luminescent and photovoltaic materials

We have developed a numerical Monte Carlo ray-tracing simulation software package of an LSC: SIMSOLAR-P. In this package, the PV cells that are attached to one or more edges of the LSC are perfect, with a current–voltage characteristic that only depends on the total flux of photons above the band-gap energy and the cell temperature. The luminescent materials are also idealized, with constant quantum efficiency, and an absorption cross section and emission power that only depend on photon energy. However, in reality there are not perfect luminescent materials nor perfect PV cells. Furthermore, most dyes are not photo stable.[8] The simple parameterizations employed here are sufficient for determining—for the first time—the theoretical limits of performance.

The organic dye combination 4-(dicyanomethylene)-2-t-butyl-6-(1,1,7,7 tetramethyljulolidyl-9 enyl)-4H-pyran (DCJTB)[9] that was studied for suitability as an LSC material[4] has demonstrated stabilities exceeding 100 years under accelerated organic light emitting diode stress tests.[10] However, the absorbance spectrum for this dye combination only covers a small region of the global solar spectrum. Recent studies of a thin film of DCJTB molecules coated on a high-index of refraction glass in a planar solar concentrator arrangement (25 × 25 × 2 mm) and a GaInP PV cell attached to one edge of the device,[4] show a relatively small power conversion efficiency. One of the highest power conversion efficiencies for a single layer device with GaAs PV cells attached to the edges and a geometrical concentration of a factor of 2.5 was measured to be 7.1%,[11] which is still small compared to current PV devices. This particular wavelength shifted photoluminescent spectrum could benefit from the use of non-conventional PV cells with band-gap energy tailored to match the characteristics of the luminescent material. The use of additional layers in the LSC with quantum nanocrystals could increase significantly the overall efficiency by segmenting the solar spectrum analogously to a tandem solar cell. In our simulations, we have studied the performance of LSCs employing the DCJTB dye and/or perfect luminescent materials in LSCs of one to three layers coupled to perfect PV cells.

Kennard-Stepanov theory

All luminescent matter must obey a thermodynamic relationship between emission and absorption called the Kennard-Stepanov (K-S) relationship.[12,13] This links the Stokes shift between emission and absorption to the overlap between emission and absorption that is responsible for the re-scattering of the fluorescent emission and a reduced efficiency. For a luminescent material modelled as a quantum system with a population of thermally equilibrated metastable excited states, the K-S theory establishes a relationship between absorption, emission and temperature:

$$ln\left(\frac{c^2}{8\pi h}\frac{I(\upsilon)}{\upsilon^3\sigma(\upsilon)}\right) = -\frac{h\upsilon}{k_B T} + D(T) \quad (1)$$

where I(υ) = emissive power spectral density at frequency υ, σ(υ) = absorption cross-section at frequency υ, k_B = Boltzmann's constant, T = temperature, c = speed of light, h = Planck's constant.

The term $D(T)$ is independent of photon energy and determined by the structure of the absorbing species:

$$D(T) = h\nu_0/k_B + \ln(Z/Z') \quad (2)$$

In this expression $h\nu_0$ is the energy shift between the ground and metastable excited state manifolds, and Z and Z′ are the partition functions of the ground and metastable manifolds, respectively.

The K-S relation requires that there will be some emission at any energy where there is absorption (and vice versa) as shown

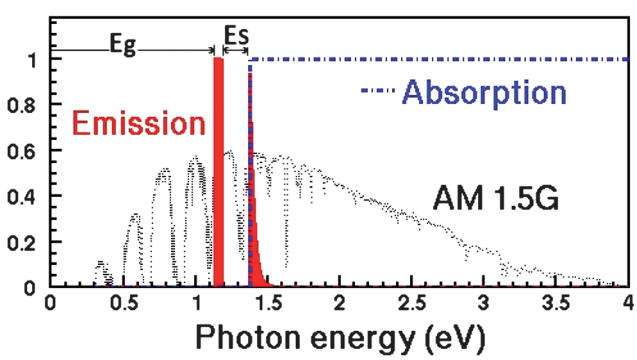

Fig. 2 Aspects of a perfect luminescent material based on the K-S equation. The emission and absorption spectrum are normalized to unity, while the standard solar global spectrum (AM 1.5G) is in [kW/eV/m²]. Eg: Energy of the band gap, Es: Stokes shift energy.

schematically in Fig. 2 for a perfect luminescent material. The objective of the global optimization is to find the optimal emissive energy and the respective energy absorption edge that provide the maximum optical efficiency for a given LSC configuration while maintaining the K-S condition. A similar approach has been recently published,[14] in which a luminescent solar spectral splitting analysis was carried out on a cylindrical concentrator. Here, however, we provide information for multi-layer solar concentrators and the ideal properties of luminescent materials for one, two and three layer LSCs.

Model of perfect luminescent matter

A perfect luminescent material in the K-S theory has uniform absorption cross section for photons above a threshold energy and constant emissive power in a narrow band from the "band-gap" energy to the emission peak energy. (The band-gap energy is so named because this is the energy to use for the band-gap of a perfect PV material to harvest the emitted light with maximum efficiency.) Because the K-S theory relates emission and absorption, there must be absorption in the perfect emission band and emission in the perfect absorption band, calculable through eqn (1). The value of D(T) is a free parameter in this model, playing the role of a normalization constant in the ratio of emission to absorption, which we parameterize as the energy of a "crossover" point where emission is equal to absorption. Thus the perfect K-S model has four parameters: the band gap energy, the width of the perfect emission peak, the absorption threshold, and the crossover energy. Fig. 2 illustrates the emission and absorption spectra for one such parameterization with the solar AM 1.5G spectra in the background. The emission peak in the perfect absorption region is an unavoidable consequence of the K-S theory. The requisite absorption in the perfect emission region is too small to see.

Numerical simulation of the LSC

We have implemented a geometrical ray-tracing model based on Monte Carlo techniques, SIMSOLAR-P, to numerically simulate planar LSCs. A distinctive feature of SIMSOLAR-P is its master-slave parallel implementation, featuring the Asynchronous Dynamic Load Balancing (ADLB) library FORTRAN interface to the Message Passing Interface (MPI) parallel programming core.[15] During the genetic algorithm optimization, the number of luminescent material configurations that integrate the population per each generation, represents a work sharing among the number of processors available in the parallel configuration. Thus, the use of ADLB reduces efficiently the computation time for the optimization of an LSC. The use of parallel processing permits us to investigate a large number of parameters (slab geometry, optical properties of the luminescent material and the matrix, incident light properties, *etc.*) in a reasonable time. We determined that ADLB resulted in an overall efficiency of approximately 90% with the simultaneous use of 60 processor nodes.

Global optimization with genetic algorithm†

A heuristic evolutionary technique known as a genetic algorithm (GA),[16] which uses a coding variable instead of the variables themselves, was chosen to determine the optimized parameters that define the limits on efficiency of a specific LSC configuration. Details are given in the Electronic Supplementary Information. The parameters for LSC efficiency are based on the K-S thermodynamic relationship between emission and absorption. As a result of the inherent Monte Carlo variance of the global optimum, the luminescent material configuration values are given within a numerical range corresponding to one standard deviation of statistical accuracy.

Results

For this study, LSC's with one or more layers with dimensions 20 × 20 × 0.5 cm were considered (typical dimensions of LSC prototypes). Perfect mirrors were attached to three sides of each layer and a perfect PV cell with band-gap energy matching the band-gap energy of the luminescent matter in its layer was attached to the fourth side. Air gaps separate each layer, and a perfect mirror was also attached to the bottom surface of the lowest layer of the LSC. The index of refraction for the concentrator was chosen to be 1.7, a value typical of high-index plastics and glasses. (We note that plastic lenses used in eyewear are commonly available with n > 1.8. The fraction of isotropic light reflected by total internal reflection is $\sqrt{1-1/n^2}$. Thus, for n = 1.7, 81% of the emitted light is contained within the LSC. For more common plastics such as PMMA with n = 1.5, the LSC would trap 75% of the emitted light.) We used a photo-luminescent efficiency of 90% for the combination dye (DCJTB)[4] and 100% for the perfect luminescent material. GA techniques were used to find the optimum model parameters for the material in each layer, its optimum concentration, and the optimum band-gaps of the PV cells.

Fig. 3 shows the optimum band-gap energy that resulted from the GA implementation for a single layer configuration with a perfect luminescent material compared to a two-layer configuration with the combination dye in the first layer and a perfect luminescent material in the second layer. Briefly, the initial generation represents a population of 60 individuals with input variables chosen randomly from the user-defined intervals. After cross-over and mutation operations are performed over the initial population, 60 new individuals are created, thereby, 60 individuals with the best fitness evaluation will comprise the next generation. The process is repeated until a convergence criterion is achieved. (More details are given in the supplement.) The band-gap energy for both configurations have similar values and

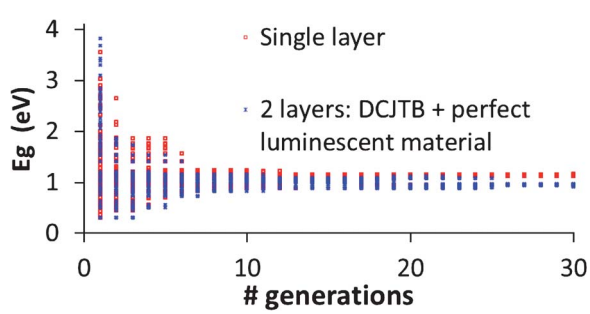

Fig. 3 Emission energy *vs.* number of generations, the values converge to the optimum emission energies after 25 generations.

This journal is © The Royal Society of Chemistry 2012

Table 1 Optimization results for multi-layer configurations with perfect luminescent materials and a dye combination (DCJTB) in the first layer. All parameters have units of eV and the efficiency η_{ave} is a percentage. The standard deviations for η_{ave} and E_g are equal to 0.2 and 0.002, respectively

LSC	1 layer (DCJTB)	2 layers	3 layers
η_{ave}	9.3	22.8	28.7
E_{g1}	1.649	1.649	1.649
E_{g2}		0.927	1.286
E_{g3}			0.730
E_{S2}		0.181 ± 0.007	0.206 ± 0.004
E_{S3}			0.185 ± 0.004
W_{e2}		0.040 ± 0.009	0.040 ± 0.004
W_{e3}			0.038 ± 0.002
E_{X2}		1.140 ± 0.003	1.524 ± 0.003
E_{X3}			0.946 ± 0.002

Table 2 Optimization results for multi-layer configurations with perfect luminescent materials. The parameter definitions, their units, and the standard deviations for η_{ave} and E_g are as in Table 1

LSC	1 layer	2 layers	3 layers
η_{ave}	21.3	29.5	33.6
E_{g1}	1.156	1.557	1.779
E_{g2}		0.902	1.154
E_{g3}			0.698
E_{S1}	0.199 ± 0.006	0.196 ± 0.006	0.202 ± 0.004
E_{S2}		0.179 ± 0.005	0.201 ± 0.006
E_{S3}			0.189 ± 0.008
W_{e1}	0.044 ± 0.008	0.057 ± 0.007	0.060 ± 0.003
W_{e2}		0.041 ± 0.005	0.034 ± 0.007
W_{e3}			0.058 ± 0.009
E_{X1}	1.380 ± 0.004	1.808 ± 0.001	2.033 ± 0.004
E_{X2}		1.117 ± 0.002	1.385 ± 0.003
E_{X3}			0.940 ± 0.002

the optimum efficiencies converge to 21 and 23% for the single layer and two-layer configurations, respectively, thus the organic dye is far from optimal for the top layer of the two layer concentrator.

Table 1 shows the optimum LSC parameters for multi-layer configurations. The uppermost layer of the LSC uses the DCJTB dye combination, and the lower layers (if any) use a perfect luminescent material with the tabulated parameters. Here, η_{ave} is the overall mean power conversion efficiency in (%) and E_g, E_S, W_e, and E_x are respectively the band gap energy, Stokes shift, emission width, and crossover point parameters of the perfect dye model in eV. For the DCJTB dye, E_g is the band-gap energy of the PV cell attached to its layer; the dye's emission and absorption spectra are static and only its concentration was allowed to vary.

The predicted optimum emission energies for a two layer concentrator as indicated in Fig. 4 suggest that near infrared materials, with typical band-gap energy of 0.9 eV, are needed for a second layer configuration. Table 2 shows the optimum LSC parameters for multi-layer configurations for perfect luminescent materials in all the layers.

Fig. 5 shows the emission energies as a function of the number of layers. The use of the global optimization permitted us to find the optimum emission energies that provide the maximum overall efficiency, which increases as a function of the number of layers.

Fig. 6 shows the overall mean power conversion efficiency for the different LSC multi-layer configurations. A value near the single-junction Shockley-Queisser limit[17] in efficiency (30%) is reached with a two-layer configuration with perfect luminescent materials and optimization converges nearly to the same Stokes-shift in all configurations (shown in Tables 1 and 2). The DCJTB dye has an effective Stokes shift of 0.46 eV and emission that peaks at 2.03 eV. These large values in comparison to the optimal values for perfect matter explains why this dye combination is not efficient for a single layer LSC, and why there is a potential for a large efficiency gain with a two layer system but not an incrementally large efficiency gain with three layers.

For perfect luminescent materials the efficiency goes from 21.3% for one layer to 29.5% for two layers and 33.6% for three layers. This can be compared to the 1 to 3 layer tandem-cell efficiency limits[18] of 30.8%, 42.9%, and 49.3%, respectively; the difference is primarily due to the loss of luminescent light that strikes the LSC faces at too small of an angle to be trapped by total internal reflection for the n = 1.7 index of refraction. Note that the three layer system exceeds the single-junction Shockley-Queisser limit. It's interesting to note that despite the many significant differences between the theoretical model and assumptions of the present work and the early work of [2], the overall conversion efficiency for our 3-layer LSC (33.6%) is comparable to their 4-layer LSC (32.0%) that absorbs the same range of the solar spectrum.

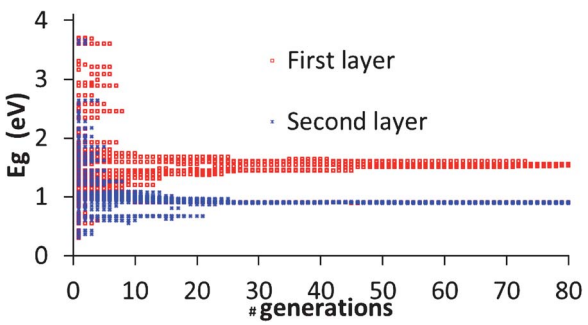

Fig. 4 Emission energies *vs.* number of generations for a two-layer configuration with perfect luminescent materials, the optimum highest value corresponds to the first layer.

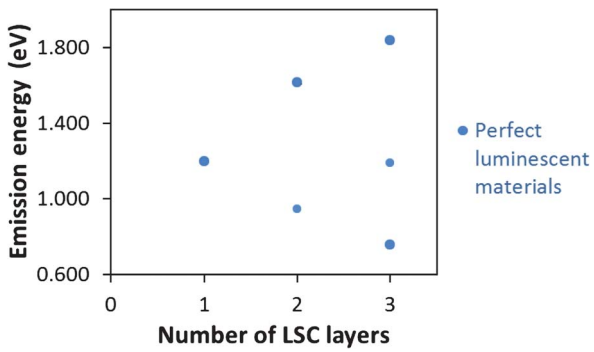

Fig. 5 Emission energies obtained for the LSC multi-layer configurations with perfect luminescent materials simulations.

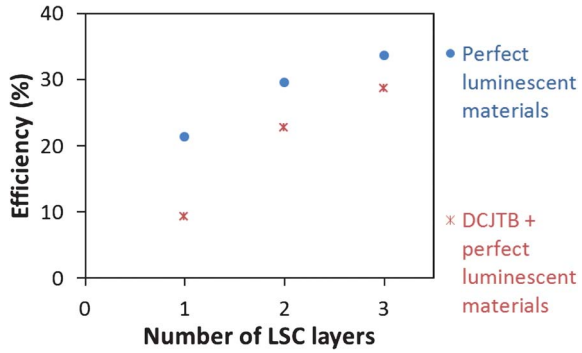

Fig. 6 Overall LSC efficiency *vs.* number of LSC layers.

Conclusions

Theoretical limits of efficiency were determined for one to three layer LSC systems; these results provide a road map for the implementation of LSCs. At least a two layer system and new photo stable luminescent materials that operate in the near infrared are necessary to boost efficiency. Under ideal conditions, a third layer does not add very significantly to the overall efficiency. Geometrical considerations such as luminescent material concentration as a function of thickness are not considered in this study because of the necessity to incorporate costs into the optimization. The next stage of this project will benchmark the Ray Tracing Model with experimental data and optimize the design using data from nanorod experiments. Finally, dye/nanorod alignment and realistic PV cell characteristics should be incorporated into the model.

Acknowledgements

We thank George Crabtree, Arnaud Demortière, Jeffrey Guest, Ewing Lusk, Matthew Pelton, Tijana Rajh, Chunxing She, Elena Shevchenko, Dmitri Talapin and Gary Wiederrecht for useful discussions. This work was partially supported by the DOE offices of Nuclear Physics and Basic Energy Sciences with contract no. DE-AC02-06CH11357.

Notes and references

1 W. H. Weber and J. Lambe, *Appl. Opt.*, 1976, **15**, 2299.
2 A. Goetzberger and W. Greubel, *Appl. Phys.*, 1977, **14**, 123.
3 W. G. H. M. van Sark, *et al.*, *Opt. Express*, 2008, **16**, 21773.
4 M. J. Currie, J. K. Mapel, T. D. Heidel, S. Goffri and M. A. Baldo, *Science*, 2008, **321**, 226.
5 D. V. Talapin, J. H. Nelson, E. V. Shevchenko, S. Aloni, B. Sadtler and A. P. Alivisatos, *Nano Lett.*, 2007, **7**, 2951.
6 D. V. Talapin, *et al.*, *Nano Lett.*, 2003, **3**, 1677.
7 J. Bomm, *et al.*, *Sol. Energy Mater. Sol. Cells*, 2011, **95**, 2087.
8 S. J. Batchelder, Ph.D. Thesis, California Institute of Techonology, 1982.
9 C. H. Chen, C. W. Tang, J. Shi and K. P. Klubek, *Macromol. Symp.*, 1998, **125**, 49.
10 M. Thompson, *MRS Bull.*, 2007, **32**, 694.
11 L. H. Sloof, E. E. Bende, A. R. Burgers, T. Budel, M. Pravettoni, R. P. Kenny, E. D. Dunlop and A. Büchtemann, *Basic Solid State Phys.*, 2008, **6**, 257.
12 E. H. Kennard, *Phys. Rev.*, 1918, **11**, 29.
13 B. I. Stepanov, *Sov. Phys. Dokl.*, 1957, **2**, 81.
14 B. Fisher and J. Biddle, *Sol. Energy Mater. Sol. Cells*, 2011, **95**, 1741.
15 E. Lusk, *et al.*, *SciDAC Rev.*, 2010, **17**, 30.
16 J. Holland, *Adaptation in Natural and Artificial Systems*, USA, 1975.
17 W. Shockley and H. J. Queisser, *J. Appl. Phys.*, 1961, **32**, 510.
18 Alexis de Vos, *J. Phys. D: Appl. Phys.*, 1980, **13**, 839.

This journal is © The Royal Society of Chemistry 2012